מכון ויצמן למדע
WEIZMANN INSTITUTE OF SCIENCE

Ph.D. Research Proposal

תוכנית מחקר לדוקטורט

By
Hagai Edri

מאת
חגי אדרי

פיסיקה מרובת חלקיקים עם בוזונים ופרמיונים קרים
Many-Body Physics with Ultracold Bosons and Fermions

Advisors:
Prof. Nir Davidson
Prof. Roee Ozeri

מנחים:
פרופ' ניר דודזון
פרופ' רועי עוזרי

February 2016

אדר א' תשע"ו

Abstract

In this proposal I report on the progress in building an experimental apparatus to produce a quantum degenerate Fermi and Bose gases of ^{40}K and ^{87}Rb (respectively). I describe two experiments that we can perform using the apparatus: measuring fermion mediated interactions between bosons in a Bose-Fermi mixture[1] and exciting a collision-less zero sound mode of a Fermi liquid [2] in a degenerate Fermi gas of ^{40}K in an elongated harmonic trap [3].

Building the apparatus is done cooperatively with Asif Sinay, Noam Matzliah and Alok Kumar Singh.

Contents

1 Experimental Setup

Our apparatus (Figure 1) consists of two vacuum cells (a MOT cell and Science cell hereafter, commonly used in the ultracold atoms community) connected by an L shaped tube that enables differential pumping and UHV in the science cell ($< 10^{-11} torr$). The vacuum is generated by a 55 liter ion pump, connected to the MOT cell and another 150 liter ion pump, connected close to the science cell. In the MOT cell we have 5 atomic sources (Alvasource non evaporative getters), two of ^{87}Rb and three of ^{40}K, these provide atoms for the experiment. They also release a lot of unwanted atoms to the cell that causes high pressure ($10^{-8} torr$) in the MOT cell.

In the MOT cell we have built a double species Magneto Optical Trap (MOT) that captures the atoms and cools them from room temperature to $\sim 300\mu K$, after compression of the cloud and further sub-Doppler cooling [4] the atoms are loaded to a magnetic trap. The magnetic trap potential is then moved over a $42cm$ L shaped tube to the science cell. That is done by running suitable currents through a chain of 15 coil pairs, thus changing the position of the magnetic trap without changing its geometry [5]. The atoms follow the trap adiabatically without significant heating of the cloud.

Our science cell is very small compared to other similar systems, it has a size of $8mm \times 8mm$ with wall thickness of $1.5mm$ (Starna). This allows us better optical access, a large numerical aperture in the imaging system and it is easier to get to UHV. On the other hand, it limits our time of flight imaging in the cell and affects the lifetime of large atomic clouds in the magnetic trap. In the science cell we trap the atoms in an optically plugged magnetic trap, this trap is a combination of a linear magnetic potential and a repulsive optical potential of a blue-detuned Gaussian beam. The blue-detuned beam is used to prevent atoms from reaching the region where the magnetic field is low. In this region the atoms can undergo non-adiabatic spin flips (known as Majorana spin flips [6]) and escape from the trap. With RF/MW induced evaporative cooling we cool the atoms to sub micro Kelvin temperature.

After the evaporation in the plugged magnetic trap we transfer the atoms to a crossed dipole trap (section 1.1) formed by two high-power laser beams. The beams wavelength ($1064nm$) is far from the atomic resonances ($766,770nm$ for ^{40}K and $780,795nm$ for ^{87}Rb). In the dipole trap the atoms are transferred to their magnetic ground state adiabaticly with a MW/RF sweep at a constant magnetic field. Measuring atomic properties is done by shining a resonant laser beam on the atoms and imaging the shadow they cast on a CCD camera (absorption imaging) or measuring the florescence signal (florescence imaging) [7].

The apparatus was designed to produce a BEC of ^{87}Rb and a degenerate Fermi gas of ^{40}K, while BEC was achieved in the plugged magnetic trap and in the dipole trap, cooling ^{40}K has been more difficult and so far we got close to the Fermi temperature but not below it.

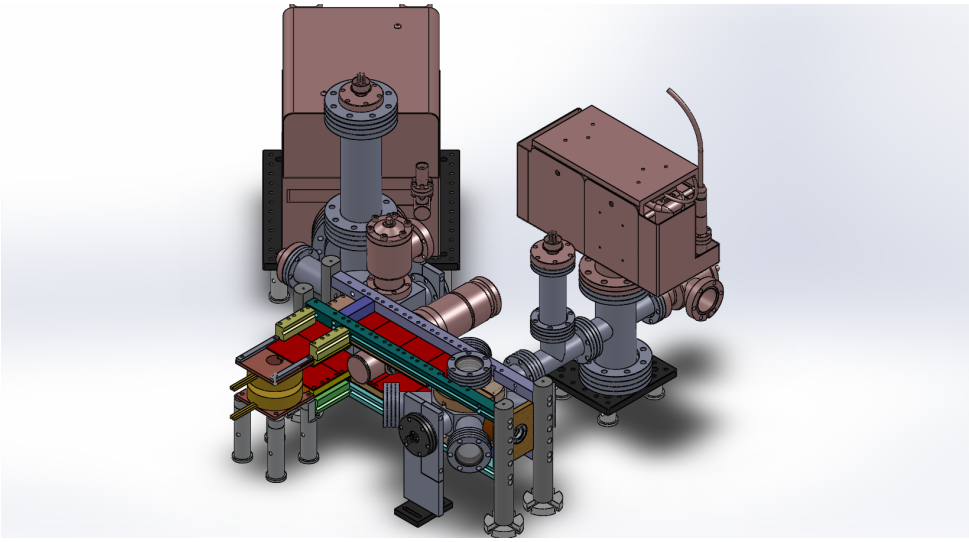

Figure 1: Experimental Apparatus - Two vacuum cells connected by an L shaped tube. Transport between the cells is done with a magnetic transport system of 15 coil pairs (in red). An all metal gate valve (VAT 48124-CE01) is placed between the cells to allow keeping a high vacuum in the science cell when replacing the atom sources. MOT cell has 6 windows for MOT beams and 5 getters of ^{87}Rb and ^{40}K that provide the atoms for the experiment. Vacuum is maintained with two Ion pumps, another titanium sublimation pump is connected but is not used.

1.1 Dipole Trap

When light with a wavelength far from atomic resonances interacts with atoms, the scattering rate is small and the dominant force is the dipole force. The electric field of the laser **E** induces an electric dipole on the atoms **d** that oscillates with the same frequency. This induced dipole then interacts with the electric field, the interaction energy is (using the rotating wave approximation) [8]:

$$U(r) = -\frac{3\pi c^3}{2\omega_0^3}\frac{\Gamma}{\Delta}I(r)\ . \tag{1}$$

Here c - is the speed of light, Δ - is the detuning frequency of the laser with respect to the atomic resonance, Γ- is the natural linewidth of excited state and I - is the laser intensity. For alkali atoms there are two transitions that need to be accounted for, the total potential is:

$$U(r) = \frac{\pi c^2 \Gamma}{2\omega_0^3}\left(\frac{2+\mathscr{P}g_f m_f}{\Delta_{2,F}} + \frac{1-\mathscr{P}g_f m_f}{\Delta_{1,F}}\right)I(r) \tag{2}$$

$\Delta_{2,F}\left(\Delta_{1,F}\right)$ - detuning frequency of the laser with respect to splitting between $^2S_{1/2,F}$ and $^2P_{3/2}\left(^2P_{1/2}\right)$, $\mathscr{P}$ - laser polarization: ± 1 for $\sigma^{\pm}$ polarization or 0 for linear polarization, g_f - Landé factor, m_f - magnetic quantum number. A red detuned Gaussian beam $(\Delta < 0)$ creates an attractive potential that traps the atoms.

In our setup the dipole potential is produced by two elliptical Gaussian beams crossing horizontally at an angle of 90° at the center of the magnetic trap. The laser is red detuned (1064

nm wavelength) and linearly polarized. The beams frequency is shifted 160 MHz with respect to each other to avoid interference. The beams come out of a single mode fiber to get a clear Gaussian mode and better stability. They pass through two cylindrical lenses that set the aspect ratio and focused at the center of the magnetic trap. Typically, each beam has a power of up to 5 Watts, their $1/e^2$ waist is $W_{0x} = 73\mu m, W_{0z} = 24\mu m$ for the beam propagating in the y direction, $W_{0y} = 77\mu m, W_{0z} = 24\mu m$ for the beam propagating in the x direction. Close to the bottom of the trap we can approximate the potential to be harmonic and measure the trap frequencies. Our trapping potential is:

$$U_{tr}(r) \approx U_0 \left(1 - 2\frac{x^2}{W_{0x}^2} - 4\frac{z^2}{W_{0z}^2} - 2\frac{y^2}{W_{0y}^2}\right) , \tag{3}$$

$U_0 = \frac{\pi c^2 \Gamma}{2\omega_0^3}\left(\frac{2}{\Delta_{2,F}} + \frac{1}{\Delta_{1,F}}\right) \cdot I_0$ (notice that $U_0 < 0$), I_0 is the maximal laser intensity of the beams (assumed equal). The trapping frequencies are $\omega_x = \sqrt{-\frac{4U_0}{mW_{0x}^2}}$, $\omega_y = \sqrt{-\frac{4U_0}{mW_{0y}^2}}$, $\omega_z = \sqrt{-\frac{8U_0}{mW_{0z}^2}}$.

Transferring the atoms to the dipole trap from the plugged magnetic trap is done adiabatically while maintaining their spin state. Then the atoms are transferred to their magnetic ground state adiabatically to avoid inelastic collisions. Further evaporation in the dipole trap is done by lowering the trap depth.

Transferring the atoms to the dipole trap is done by lowering the current in the magnetic trap coils and turning off the optical plug while increasing the dipole trap beams power and applying a constant magnetic field of $\sim 1G$ to keep their spin state unchanged. This is done in $\sim 200ms$ when the cloud is cold and dense in the magnetic trap. After trying it at several stages of the RF evaporation and it was found that the optimized time to transfer is when the cloud is colder than 10 μK. At this time the cloud is small enough to be contained in the center of the dipole trap, and the trap depth is sufficient to capture most atoms. Transferring the atoms at lower temperatures is inefficient since there is always some heating in the process. Immediately after that a MW (RF) is used sweep to transfer the ^{87}Rb $\left(^{40}K\right)$ to the ground state $|1,1\rangle$ $\left(|\frac{9}{2}, -\frac{9}{2}\rangle\right)$ in $30ms$, this is done to avoid inelastic collisions that will lead to losses and a short lifetime in the trap (~300 ms). We measured a lifetime $\tau > 60s$ in the dipole trap after the MW/RF transfer indicating low collision rate with background gas and ultra high vacuum conditions.

Trapping frequencies are an important parameter in our experiment, they give a typical time scale for the atoms movement, they set the Fermi energy (for fermions) and the critical temperature for BEC (for bosons). To measure the trap frequencies there are two standard techniques:

- Perturbing the atomic motion in the trap - Applying a weak force on the atoms for a short time causes the atoms to oscillate in the trap at the trap frequencies. Looking at the center of mass position of the cloud at different times, the oscillation frequency can be inferred.

- Parametric excitation - Changing the trapping potential in a periodic way to excite oscillations in the cloud size and cause heating. Measuring heating or loss of atoms after

excitation for different frequencies shows a resonance response at $\omega = 2\omega_{trap}$.

The trap frequencies were measured by center of mass oscillations (Figure 2) and validated by parametric excitation. To excite center of mass oscillations in the horizontal directions a magnetic force was applied by turning on a magnetic field gradient for a short time with our Stern-Gerlach apparatus (see section 1.3). To excite center of mass oscillations in the vertical direction the trap beams were turned off for a short time, letting the cloud free-fall for some time, and then the beams were turned on to re-trap the atoms. To evoke parametric excitation the power of one of the beams was modulated sinusoidally and the loss of atoms after $\sim 1s$ in the trap was measured . Scanning the frequencies a significant loss was seen at the resonance of the cloud expansion mode ($\omega = 2\omega_{trap}$). Comparing the calculated frequencies to the measured ones , we had a good agreement with the calculations (Figure 3).

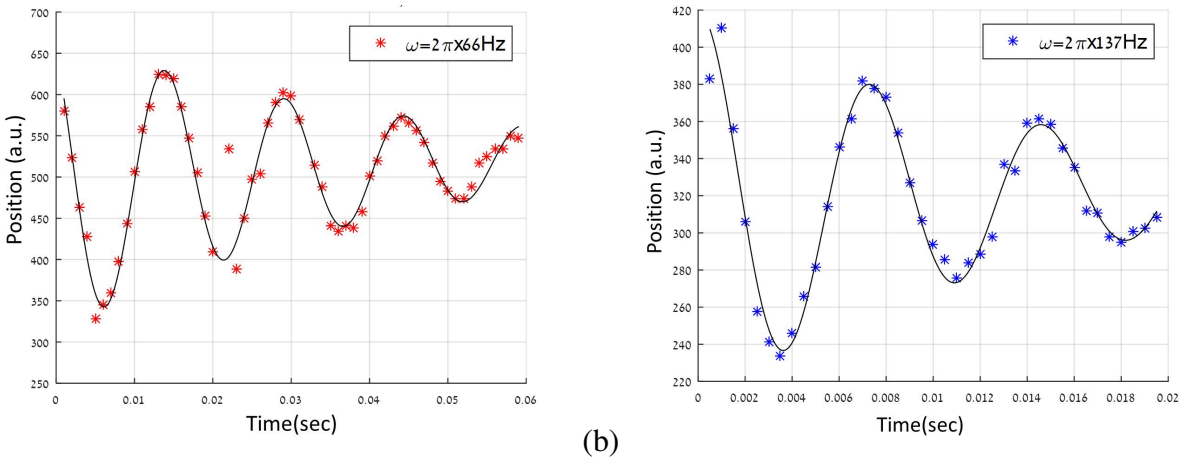

(a) (b)

Figure 2: Oscillations in Dipole Trap - Atomic center of mass oscillations in horizontal (a) and vertical (b) directions, with a fit to exponentially decaying oscillations (black). The cloud was imaged after release from the trap.

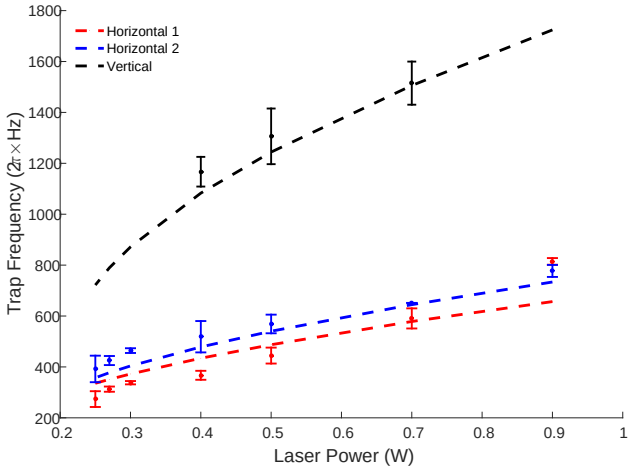

Figure 3: Dipole Trap Frequencies - Comparison of the calculated frequencies (dashed lines) to the measured frequencies from the center of mass oscillations in the dipole trap. For three trap axes and different dipole trap beams power.

1.1.1 BEC in Dipole Trap

Producing a BEC in the dipole trap is carried out by evaporative cooling in the plugged magnetic trap to low temperatures ($T < 10\mu K$), transferring the atoms to dipole trap adiabatically, changing their spin-state to the ground state and performing evaporative cooling by slowly decreasing the trap depth (lowering the trap beams power).

^{87}Rb atoms are loaded in the dipole trap and transferred to the atomic ground state, and after 4 seconds of evaporation a BEC of $\sim 3 \cdot 10^5$ atoms is achieved. The clearest indication of BEC is the appearance of a sharp peak in the atoms distribution a long time after they are released from the trap, this shows the macroscopic occupation number of the ground state of the system. These atoms have low momentum and they don't expand during the time of flight. Figure 4 shows the column density of the cloud after $20ms$ time of flight at different stages of the evaporation. A central peak is observed and it increases as we continue the evaporation further. Using a bimodal fit of a BEC and a thermal cloud we can get the cloud temperature, atom number and condensate fraction.

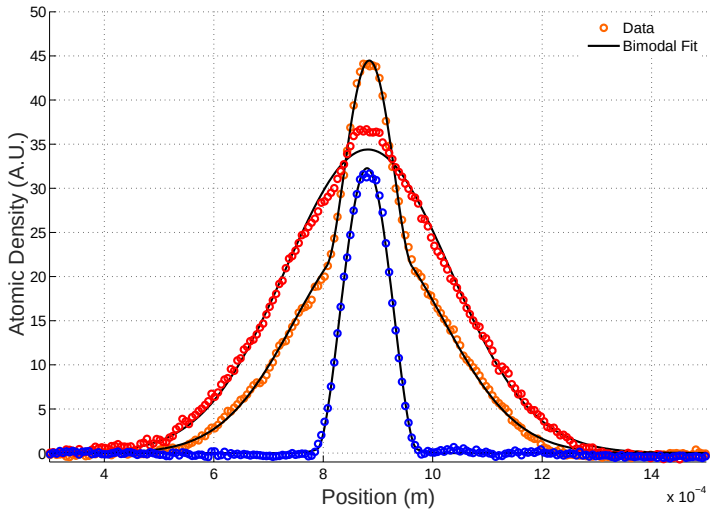

Figure 4: BEC in the Dipole Trap - Column densities of the cloud after 20ms time of flight. Lowering the trap depth increases the number of atoms in the condensate. The cloud evolves from a thermal cloud (red circles) to an almost pure condensate (blue), a bimodal distribution is clearly visible (yellow circle). Using a bimodal fit (black lines) [9] the condensate fraction and temperature can be extracted.

The calculated condensate fraction and temperature are used to fit the data to theory (Figure 5) [10]. For a non-interacting gas in an harmonic trap the condensate fraction should be: $\frac{N_0}{N} = 1 - \left(\frac{T}{T_c}\right)^3$, $\frac{N_0}{N}$ is the condensate fraction, T is temperature and T_c is the critical temperature for BEC. For an interacting gas two models are presented [11], showing that interactions play a crucial part in our system.

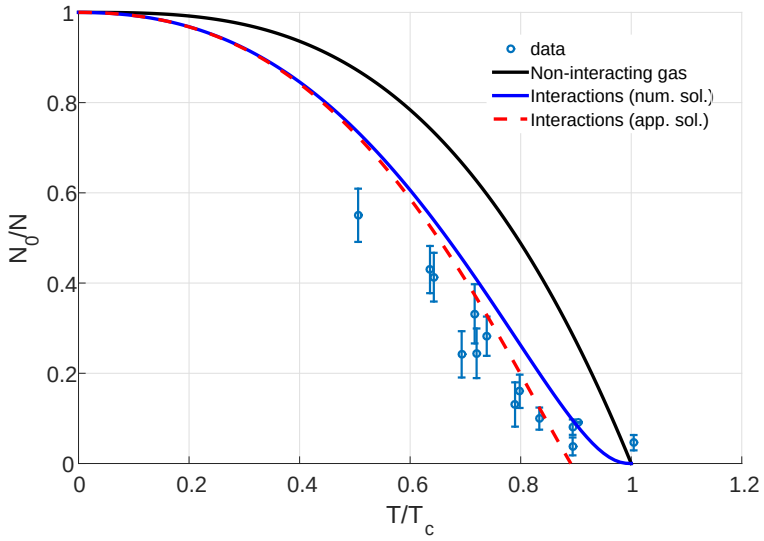

Figure 5: Phase Transition - Condensate fraction $\frac{N_0}{N}$ increases as the cloud is cooled further below the critical temperature T_c. The measured data is compared to the non-interacting case $\frac{N_0}{N} = 1 - \left(\frac{T}{T_c}\right)^3$ (black) and two models that account for interactions (blue and red) [11].

1.2 Sympathetic Cooling of ^{40}K

After successfully producing BEC of ^{87}Rb in the plugged magnetic trap with RF evaporation it seemed reasonable a degenerate Fermi gas of ^{40}K can also be produced, however, sympathetic cooling proved to be a difficult challenge that we have not yet managed to overcome.

Evaporative cooling is an effective way to cool atomic clouds and get to quantum degeneracy. A cloud of atoms in a trap is cooled when the hottest atoms are allowed to escape the trap. Each atom that leaves the trap carries away more than the average energy. The remaining atoms re-thermalize by elastic collisions and acquire a new, lower temperature. RF induced evaporative cooling [12] is used to induce transition between trappable ($g_f m_f > 0$) and untrappable states ($g_f m_f < 0$) with radio frequency (RF) radiation. When an atom is radiated with RF radiation at a frequency that corresponds to the Zeeman splitting between two Zeeman states with $\Delta m_f = 1$ it can be transferred to a different magnetic state. If that state is untrappable then the atom will be removed from the trap. Starting with high frequencies (compared to the cloud temperature) and reducing the RF frequency in the process we can remove only the hottest atoms at each step and the cloud is cooled. This method is energy selective because only high energy atoms reach the regions in the trap corresponding to high magnetic fields and high Zeeman splitting energy, thus only those atoms are affected by the RF radiation. It allows us to keep the trap constant during the evaporation, and the process is easily controlled by the amplitude and frequency of the RF radiation.

In a $^{87}Rb - ^{40}K$ mixture trapped in a magnetic trap it is possible to remove only the ^{87}Rb atoms because the Zeeman splitting of ^{40}K in the state $\left|F = \frac{9}{2}, m_f = \frac{9}{2}\right\rangle$ is larger by a factor

~ 2.25 than that of ^{87}Rb at the same magnetic field, so the ^{40}K atoms will not interact with the RF radiation and they remain trapped. Sympathetic cooling is based on the assumption that the ^{40}K atoms collide with the ^{87}Rb and the clouds maintain a thermal equilibrium throughout the evaporation by colliding with each other (the ^{40}K gas is spin polarized and they do not collide with each other due to Pauli exclusion principle). Therefore, when we cool the ^{87}Rb by RF induced evaporative cooling the ^{40}K cloud also gets colder, and the number of ^{40}K remains unchanged as only the ^{87}Rb atoms are removed from the cloud. Other groups working with a mixture of $^{87}Rb -^{40} K$ have successfully done that and lost only a small part of the ^{40}K cloud (it decreased by a factor $2-10$, compared to a factor of 10^3 of the ^{87}Rb atoms) [13, 14, 15].

In our first attempts it was seen (Figure 6 (a)) that this is not the case in our system. The number of ^{40}K is constant at the beginning of the evaporation but then it starts dropping and losses become significant. After completing the RF evaporation and another stage of evaporation in the dipole trap we only got to a ^{40}K cloud with $T \sim 1.5T_F$ (Figure 6 (b)) and it could not be cooled below the Fermi temperature to quantum degeneracy.

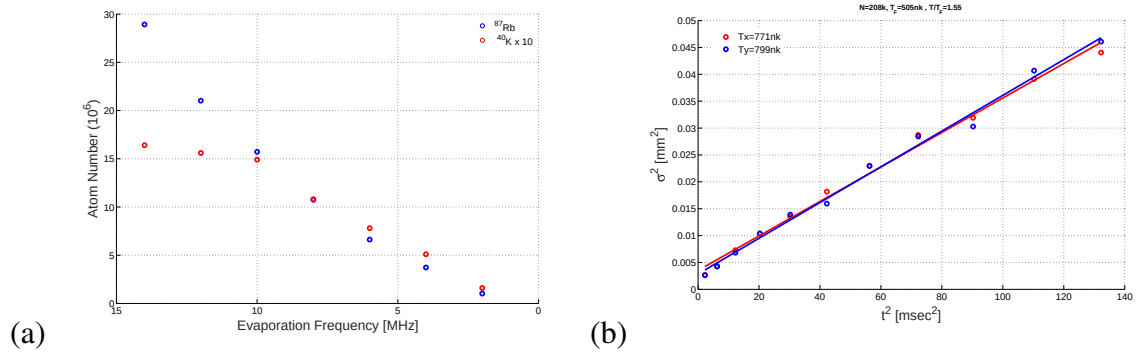

(a) (b)

Figure 6: Sympathetic Cooling - (a) Number of atoms during RF evaporation in the optically plugged magnetic trap. Showing a loss of ^{40}K atoms when evaporation frequency is below$10\dot{M}Hz$. This indicates that sympathetic cooling is not working properly. (b) Expansion of ^{40}K cloud after release from the trap, the temperature is calculated from a linear fit[9]. After evaporation in the magnetic trap and dipole trap the ^{40}K gas is close to quantum degeneracy $T \sim 1.5T_F$. T_F is the Fermi temperature, calculated from the trap frequencies and the number of atoms.

Trying to optimize the evaporation process again didn't help much and the loss of K atoms was critical. Looking at the spin states of the K atoms after transferring them to the dipole trap (using a Stern Gerlach method, Figure 8 (a)) showed that they were distributed over many spin states, this can cause in-elastic losses during the evaporation and also allow the K atoms to reach higher magnetic fields in the trap where the RF radiation will remove them from the trap (the trap is tighter for atoms with higher m_f). As mentioned before, the atoms were distributed over many spin states because a fast and sharp peak in the current of the magnetic trap coils as the atoms reach the Science cell. After fixing this problem we tried evaporating with MW radiation to avoid inducing any RF transitions on the ^{40}K atoms. MW radiation induces transitions on the hyper-fine splitting of ^{87}Rb at 6.8 GHz, which is much larger than the hyper-fine splitting

of ^{40}K at 1.2 GHz. With these improvements the number of ^{40}K atoms was much better and we got ~3 million atoms at $\sim 100\mu K$. However at that point there is a huge decrease in the cross section of $^{87}Rb-^{40}K$ due to a Ramsauer-Townsend minimum and the cooling efficiency drops [16]. To circumvent this problem we need to evaporate for a long time, this cannot be done in the optically plugged magnetic trap since the lifetime is too short (~10s). Measuring the lifetime in the optically plugged magnetic trap at different stages of the evaporation showed that the lifetime for colder clouds is shorter. Colder atoms are closer to the magnetic field minimum ($\sim 0.2\ G$), where the Zeeman splitting is smaller. This suggested that noise at low frequencies ($\sim 100kHz's$) is causing spin flips and the colder atoms are removed from the trap. Another group using an optically plugged magnetic trap reported a similar problem [17] . To avoid this problem we had to make a trap that has a higher magnetic field at its minimum.

1.3 Stern-Gerlach Measurements

Atomic spin state is characterized be F - the total angular momentum of the atom (nuclear spin, electron spin and orbital angular momentum) and m_f - the projection of F on the quantization axis. One way to measure spin states is using MW/RF spectroscopy, a different approach is applying a magnetic field gradient to separate different spin states during free expansion of the cloud. The magnetic gradient invokes a force on the atoms that depends on their spin state - $F_m = g_f m_f \mu_B \nabla B$,μ_B- Bohr magneton, g_f - Landé factor. This method is similar to the one used by Stern and Gerlach (SG) in their famous experiment to measure the spin of the electron [18]. Applying this force for a few milliseconds gives a kick to the atoms that is proportional to $g_f m_f$, thus separating different states in space. We use a circular coil with inductance $20\mu H$ and resistance 0.2Ω made of 30 turns of rectangular copper wire. The coil has an average radius $2cm$, it is placed 4.5 cm away from the cloud center. It is connected to two charged capacitors ($37mF$ each) charged to $5-30\ Volt$. Opening a fast switch (IGBT CM400HA-24H) discharges the capacitors and currents of $150-200\ A$ flows in the coil for a short time ($1-5ms$) with very short rise time ($< 0.1ms$), generating a magnetic gradient at the position of atoms. Applying this force when the cloud is trapped causes center of mass oscillations in the trap (see section 1.1). Applying it when the cloud is free-falling separates different spin states in space. Imaging the separate clouds after a long time of flight, allows us to measure the population in different spin states. In order to have a clear separation we need cold clouds such that their size is smaller than their center of mass distances after time of flight.

Stern-Gerlach measurements of ^{87}Rb after release from the dipole trap (Figure 7) show that the MW and RF change the state of the atoms, the transfer efficiency is high and the applied force is proportional to $g_f m_f$. The ^{87}Rb cloud is transferred to the dipole trap in an almost pure state after RF evaporation in the magnetic trap.

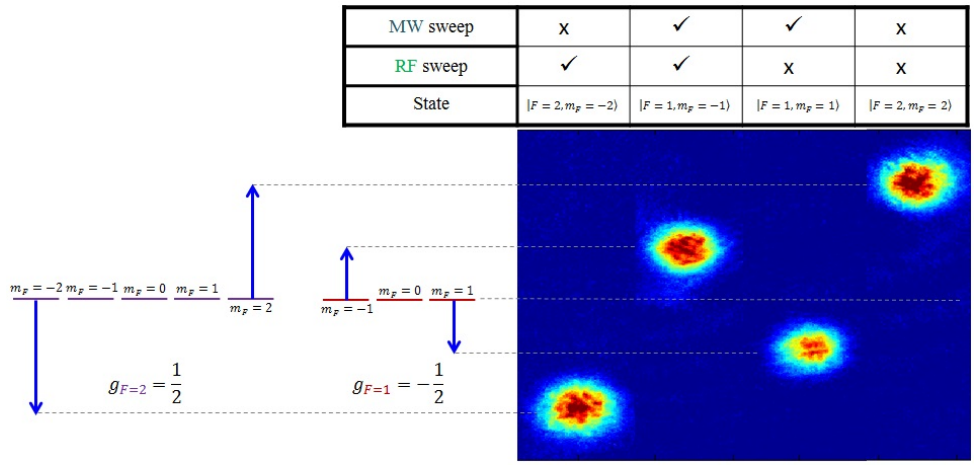

Figure 7: Stern-Gerlach Measurements of ^{87}Rb - Atomic clouds images after a long time of flight, the magnetic force excreted on the atoms during expansion moves the cloud according to its state with a force $F \propto g_f m_f$. MW sweep changes the hyper-fine state F (with different g_F) and RF sweep changes the magnetic state m_f .

Our first SG measurements of the ^{40}K cloud in the dipole trap (Figure 8 (a)) showed that the cloud is a mixture of at least 5 different spin states. This is unwanted as it leads to inelastic collisions and loss, both in magnetic and dipole traps. This was caused due to a fast and sharp peak in the current in the magnetic trap coils that took place as the atoms reached the science cell. The power supply for the trap coils produced this sharp peak when it was increasing its current from zero to a constant value. This current problem creates a fast strong change in the magnetic field that changes the magnetic state of the atoms. It was one of the reasons we did not reach degenerate Fermi gas. After fixing this problem we repeated this SG measurement in the dipole trap and a pure magnetic state and good transfer efficiency with RF sweep (Figure 8 (b)).

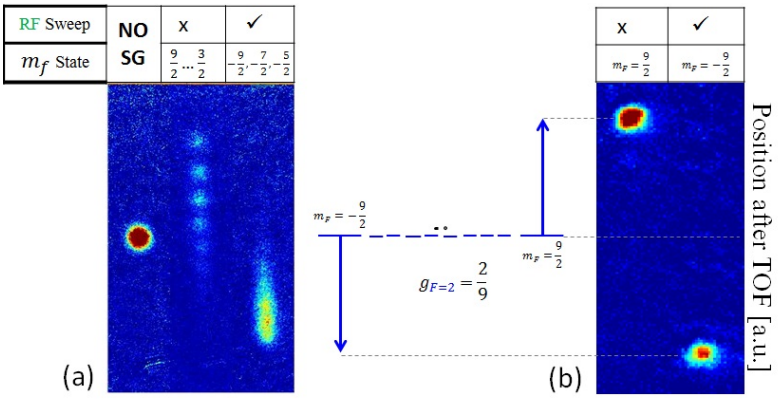

Figure 8: Stern-Gerlach Measurements of ^{40}K - Atomic clouds images after a long time of flight, the magnetic force excreted on the atoms during expansion moves the cloud according to its state. In (a) it is seen that the cloud is a mixture of 5 states, this is due to a technical problem with the current in the magnetic trap coils. (b) Was measured after fixing the problem, and it a shows a pure state, and high efficiency of changing the magnetic state with an RF sweep.

1.4 Time Orbiting Potential

A Time Orbiting Potential (TOP) trap is based on a quadrupole trap potential which is periodically orbiting in a circle around its static center. It was used to create the first BEC in 1995 [19] . For a high enough orbiting frequency f_{TOP} the atoms can not follow the orbiting field and their motion will be governed by the potential averaged over time. The averaged potential has a region around its minimum where its approximately harmonic and the magnetic field there is never zero. Thus avoiding Majorana losses, and in our case it also prevents the losses due to magnetic noise in the lab at low frequencies by increasing the Zeeman splitting at the minimum to a higher value (typically a few MHz). The TOP orbiting frequency should be higher than the harmonic trap frequency and lower than the Larmor frequency of the atoms in the trap. Under these conditions, the atoms will be trapped in the averaged potential and no spin flips will occur. Typically the trap frequencies are on the order of $\sim 100Hz$ and the Larmor frequency is about $0.5-30\,MHz$, so f_{TOP} should be a few kHz.

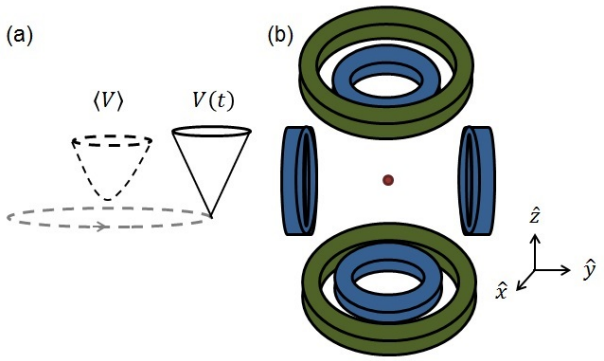

Figure 9: Time Orbiting Potential - (a) Averaging on the orbiting potential $V(t)$ creates an harmonic potential with a non-zero bias field $\langle V \rangle$. (b) Our TOP trap configuration, the quadrupole coil (green) is in Anti-Helmholtz configuration, creating a linear magnetic trap. The TOP coils (blue) are in Helmholtz configuration, creating a constant magnetic field at the center that shifts the linear potential periodically.

A magnetic TOP trap is composed of three pairs of coils (Figure 9). One pair is in the Anti-Helmholtz configuration (z axis - green in Figure 9) and it creates a linear quadrupole potential. The two other pairs are in the Helmholtz configuration in two different axes (z and x in our trap - blue in Figure 9) and they create a constant magnetic field at the center of the quadrupole potential. Adding a constant magnetic field to the linear potential shifts its center. To get a time orbiting potential, the current in the two Helmholtz pair is changed sinusoidally with a phase shift of $\frac{\pi}{2}$ between the pairs. The linear potential is than shifted alternately in the two directions without passing through the center so the atoms are never in a zero magnetic field, averaging over this motion gives the TOP trap. The magnetic field around the center of the coils in this

configuration is:

$$\vec{B}(t) = \begin{pmatrix} B'x + B_{0x}\sin\omega t \\ B'y \\ -2B'z + B_{0z}\cos\omega t \end{pmatrix}, \tag{4}$$

B' is the magnetic gradient created by the Anti-Helmholtz pair, B_{0x}, B_{0z} are the maximal magnetic fields created by the two Helmholtz pairs, $\omega = 2\pi \times f_{TOP}$ is the angular frequency of the orbiting potential. The time averaged potential is:

$$V_{TOP}(r) = \mu_B g_f m_f \left\langle \left| \vec{B} \right| \right\rangle, \quad \left\langle \left| \vec{B} \right| \right\rangle = \frac{\omega}{2\pi} \int_0^{\frac{\omega}{2\pi}} \left| \vec{B} \right| dt \tag{5}$$

for $B_{0z} = B_{0x} = B_0$:

$$V_{TOP}(r) = \mu_B g_f m_f \left[B_0 + \frac{B'^2}{4B_0} \left(x^2 + 2y^2 + 4z^2 \right) \right] \tag{6}$$

In our trap the magnitude of the fields is not equal ($B_{0z} \neq B_{0x}$), and we don't generate a pure sine wave in both directions due to technical limitations. This makes the calculations a little more cumbersome but the principle is the same.

A main disadvantage of the TOP trap is its limited trap depth compared to a quadrupole trap. The position of the zero magnetic field point is orbiting in a ellipse with $R_z = \frac{B_{0z}}{2B'}$,$R_x = \frac{B_{0x}}{B'}$, atoms crossing that ellipse can undergo a spin flip and be lost from the trap. This sets the trap depth to be $U_{max} = \mu_B g_f m_f \frac{B_0}{4}$ [9] (for a symmetric TOP trap). This means we need to transfer the atoms from the quadrupole trap to the TOP trap after some evaporation. Our TOP coils parameters are in table 1.

Coil Pair	Turns	Diameter	Width	L	R	Mag. Field @ Center
$\hat{x}$ axis (horizontal)	104	$24.5 - 65mm$	$110\ mm$	$700\ \mu H$	$365\ m\Omega$	$3.5\frac{G}{A}$
$\hat{z}$ axis (vertical)	46	$12.3 - 24.5mm$	$29\ mm$	$20\ \mu H$	$60\ m\Omega$	$4.2\frac{G}{A}$

Table 1: TOP coils parameters

10^7 atoms were loaded to the TOP trap at a temperature of $35\mu K$, loss and heating during the transfer were not significant. We measured a lifetime of $\tau_{TOP} = 96s$ in the TOP trap (figure 10) and a minimal bias field $B_0 = 38\ G$ which strongly suppresses the influence of noise at low frequencies ($100kHz$) on the atoms. Evaporation in the TOP is our next stage and should be done soon.

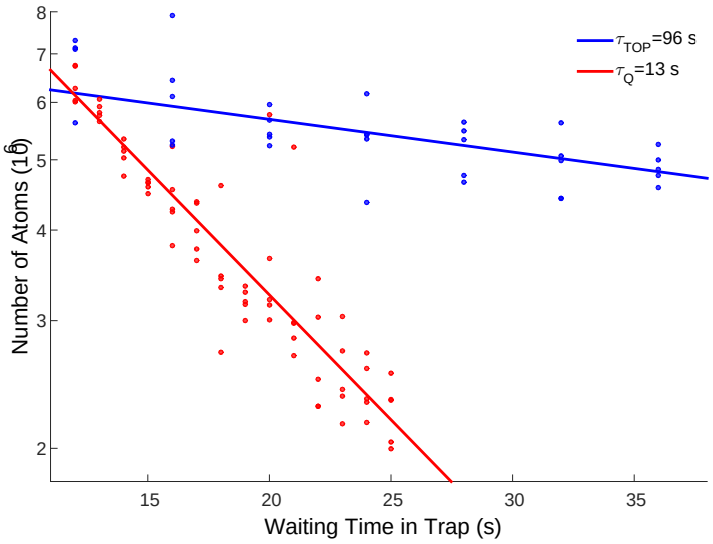

Figure 10: Life Time in TOP trap - Measuring the number of atoms in the trap for different holding times in the TOP (Blue) and quadrupole (red) trap. The measurements are noisy but still show a clear difference between the traps. The cloud is loaded to the TOP after 10s of MW evaporation in the quadrupole trap at a temperature of $32\mu K$.

2 Proposed Experiments

2.1 Fermion Mediated Interactions

Interactions in an ultracold boson-fermion mixture are manifested by elastic collisions. In a system of a dilute thermal Bose gas (^{87}Rb) and spin polarized degenerate Fermi gas (^{40}K), the collisions between the bosons and fermions can lead to an effective long-range interaction between the bosons, analogous to Ruderman–Kittel– Kasuya–Yosida (RKKY) interaction in solids [20, 21, 22]. Following [1] a 2nd order perturbation theory for this interaction is presented, along with some possible measurable quantities for a boson-fermion mixture in a 3D harmonic trap.

Similar to [1], consider a system of two bosonic atoms (^{87}Rb) immersed in a polarized degenerate Fermi gas of ^{40}K at $T=0$, the non-interacting state of the system is $|g\rangle = |\Psi_B(k_1,k_2)\rangle \bigotimes |\Psi_{DFG}\rangle$ with energy $E_g = \frac{\hbar^2\left(k_1^2+k_2^2\right)}{2m_B} + \frac{3}{5}N_F\varepsilon_F$, $k_{1,2}$ are the bosons momenta ,m_b - boson mass , N_F, ε_F are the fermion number and Fermi energy. The spin polarized fermions do not interact between themselves at low temperature due to Pauli exclusion principle, however, they can collide with one of the bosons, creating a particle-hole excitation of the Fermi gas which can propagate and interact with the second boson. This process gives rise to an effective potential between the bosons.

The boson-fermion $\left(^{87}Rb - ^{40}K\right)$ and boson-boson$\left(^{87}Rb - ^{87}Rb\right)$ collisions are described by a contact interaction Hamiltonian:

$$\hat{H}_{BF} = g_{BF}\int d^3r \psi_b^\dagger(r)\psi_f^\dagger(r)\psi_b(r)\psi_f(r) \tag{7}$$

$$\hat{H}_{BB} = \frac{g_{BB}}{2}\int d^3r \psi_b^\dagger(r)\psi_b^\dagger(r)\psi_b(r)\psi_b(r) \tag{8}$$

where $g_{bf} = 2\pi\hbar^2 a_{bf}\left(\frac{1}{m_{Rb}}+\frac{1}{m_K}\right)$, $g_{bb} = \frac{2\pi\hbar^2}{m_{Rb}}a_{bb}$, a_{bf} (a_{bb}) is the boson-fermion (boson-boson) s-wave scattering length and $\psi_b^\dagger\left(\psi_f^\dagger\right)$ are the boson (fermion) creation operators. The effective Hamiltonian describing the mediated interaction is:

$$H' = \sum_{\left\{k_1,k_2,k_1',k_2'\right\}} |g\left(k_1,k_2\right)\rangle \left[\sum_{|e\rangle}\frac{\langle g|\hat{H}_{BF}|e\rangle\langle e|\hat{H}_{BF}|g\rangle}{\left(E_e-E_g\right)}\right]\left\langle g\left(k_1',k_2'\right)\right| \tag{9}$$

The sum over $\{k_1,k_2,k_1',k_2'\}$ is when the fermions are in their ground state $|\Psi_{DFG}\rangle$, and the sum over states $|e\rangle$ is when the fermions are in an excited state. After calculating the sums (for details see [1]) the effective interaction and potential are:

$$H' = \frac{1}{2}\int d^3\left\{r_1,r_2\right\}\psi_b^\dagger(r_1)\psi_b^\dagger(r_2)V\left(r_1-r_2\right)\psi_b(r_2)\psi_b(r_1) \tag{10}$$

$$V(R) = -\frac{2m_f g_{bf}^2 k_F^4}{\hbar^2} \frac{\sin(2k_F R) - 2k_F R \cdot \cos(2k_F R)}{(2k_F R)^4} \tag{11}$$

m_f is the fermion mass and $k_F = \frac{\sqrt{2m_F \varepsilon_F}}{\hbar}$ is the Fermi momentum . This potential is shown in figure 11 and is identical to the RKKY interaction in solids.

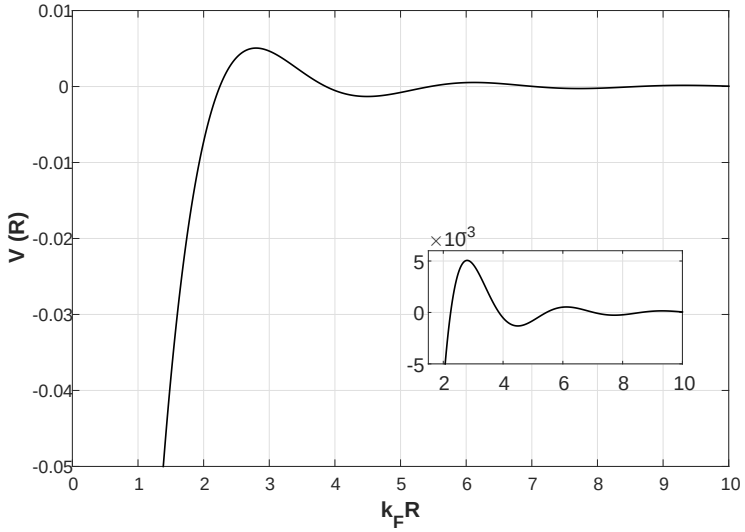

Figure 11: Fermion Mediated Boson-Boson Interaction - Mediated potential in arbitrary units, R is the distance between bosons. Inset focuses on oscillations.

In our experiment the mixture is held in a 3D harmonic trap at sub-micro Kelvin temperature. When the de-Broglie wavelength λ_{dB} of the bosons is much longer than the potential range $\sim (2k_F)^{-1}$ than to first order we can replace the RKKY interaction with a contact potential $V(R) = g_{ef}\delta(r)$, with the parameters I used for estimating the interactions $2k_F\dot{\lambda_{dB}} \sim 8$. When $g_{ef} = \int d^3R V(R)$ is the effective mediated boson-boson coupling and a_{ef} is the effective scattering length:

$$g_{ef} = \frac{4\pi\hbar^2}{m_B} a_{ef}, \quad a_{ef} = -\frac{1}{32k_F}\frac{m_b}{m_f}\left(\frac{g_{bf}k_F^3}{\varepsilon_F}\right)^2 \tag{12}$$

The scattering length is proportional to $n_f^{\frac{1}{3}}$ and to $-a_{bf}^2$, thus it is always attractive. For two bosons in different spin states $(e.g. \quad \uparrow,\downarrow)$ the interaction will be $g'_{\downarrow\uparrow} \propto g_{\downarrow f} \cdot g_{\uparrow f}$ which can be repulsive or attractive, depending to the signs of the boson-fermion interaction $g_{\downarrow f}$, $g_{\uparrow f}$.

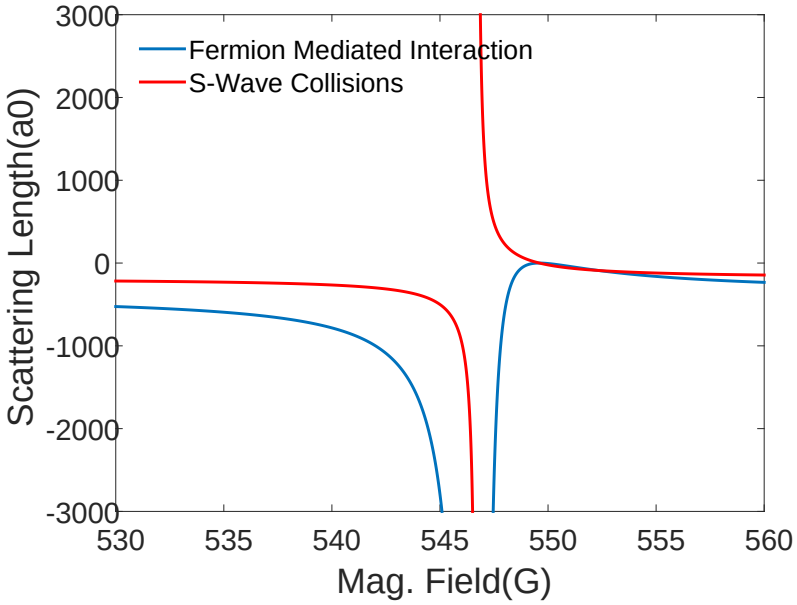

Figure 12: Scattering Length Near a Feshbach Resonance - Boson-fermion (red) and fermion mediated interaction (blue) scattering length near a boson-fermion Feshbach resonance at 546.7 G with a width $\Delta B = 2.9G$ [23].

The effect of the mediated interaction can be measured in two ways:

- Measuring the frequency shift of the ^{87}Rb Hyper-fine transition - this transition is shifted due to interactions, the effect of the mediated interaction between the bosons should cause an additional shift.
- Measuring the collision rate of the ^{87}Rb - the mediated collisions should lead to faster thermalization time and the cross section for boson-boson mediated collision should be proportional to $a_{ef}^2 \propto a_{bf}^4$.

There are three main parameters that change these effects: fermion density, boson density and the bare boson-fermion scattering length a_{bf} (can be tuned using a Feshbach resonance [23]). In the following I estimate the frequency shift and collision rate for different fermion\boson densities at zero magnetic field for the transition $\left|F=1,m_f=0\right\rangle \rightarrow \left|F=2,m_f=0\right\rangle$, it has no first-order Zeeman shift at low magnetic fields and therefore is less sensitive to magnetic noise. Close to a boson-fermion Feshbach resonance at 546.7 G I estimate the frequency shift and collision rate for the transition $\left|F=1,m_f=1\right\rangle \rightarrow \left|F=2,m_f=2\right\rangle$.

Frequency Shift

Interactions between atoms cause mean-field frequency shifts to hyper-fine transitions in alkali atoms [24, 25], the addition of another interaction term should cause additional frequency shift that can be measured by Rabi or Ramsey spectroscopy [26] on the hyper-fine transition, which

is known with great accuracy [27]. I estimate the mean-field shift of the transition between two hyper-fine states of the bosons. The mean-field shift due to the interaction of each state is:

$$\delta\mu_1 = \alpha_{bb} g_{bb_1} n_b + g_{bf_1} n_f + \alpha_{bb} g_{ef_1} n_b \tag{13}$$

$$\delta\mu_2 = \alpha_{bb} g_{bb_2} n_b + g_{bf_2} n_f + \alpha_{bb} g_{ef_2} n_b \tag{14}$$

the transition frequency shift is:

$$\frac{\delta\mu_2 - \delta\mu_1}{h} = \frac{1}{h}\left(g_{bf_2} - g_{bf_1}\right) n_f + \frac{1}{h}\left(g_{ef_2} - g_{ef_1}\right) n_b \alpha_{bb} + \frac{1}{h}\left(g_{bb_2} - g_{bb_1}\right) n_b \alpha_{bb} \tag{15}$$

g_{bb_i}, g_{bf_i}, g_{ef_i} are the boson-boson, boson-fermion and mediated interaction strength of the two hyper-fine states respectively and α_{bb} is the boson-boson two particle zero separation correlation (either 1 or 2 depending on the spectroscopy method used). From the equation it is seen that a difference between the interaction strength of the two states causes the additional shift, there are three ways to change the frequency shift:

- Changing the density of fermions n_f - the boson-fermion and mediated interations depend on n_f while the boson-boson interaction isn't.
- Changing the density of bosons n_b - the boson-boson and mediated interations depend on n_b while the boson-fermion interaction isn't. The dependence of the boson-boson interaction on n_b is weak and well known since the transition $|1,0\rangle \rightarrow |2,0\rangle$ is used in atomic clocks [28].
- Changing the boson-fermion scattering length - Using a Feshbach resonance one can tune the interaction strength for the initial state such that $g_{bf_1} \rightarrow \infty$ and then $g_{ef_1} \propto -g_{bf_1}^2 \rightarrow -\infty$. This will effect the frequency shift significantly.

To estimate the frequency shift in the three cases above I assumed a 10% difference between g_{bf_1} and g_{bf_2} and a 5% difference between g_{bb_1} and g_{bb_2} [29] at zero magnetic field (far from any Feshbach resonance) and calculated it for different fermion and boson densities that should be relevant in the experiment (Figure 13). The bosonic cloud is above the critical temperature for BEC.

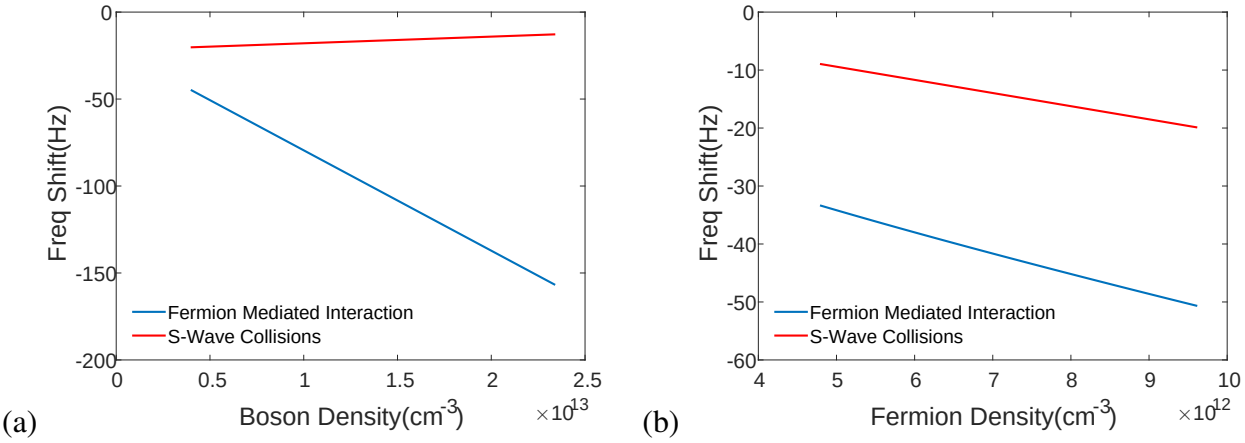

Figure 13: Mean-Field Frequency Shift at Zero Magnetic Field - Frequency shift for the rubidium $|1,0\rangle \rightarrow |2,0\rangle$ transition at zero magnetic field. (a) Frequency shift for different boson densities, fermion density is set at $9.6 \times 10^{12} cm^{-3}$. (b) Frequency shift for different different fermion densities, boson density is set at $5 \times 10^{12} cm^{-3}$. Both graphs show calculations with fermion mediated interaction (blue) and without (red). .

Close to a boson-fermion Feshbach resonance (figure 14) the frquency shift is increased as the resonance is only relevant to one of the states, to estimate it I used the zero magnetic field scattering length for state $|2,2\rangle$ and changed the magnetic field of state $|1,1\rangle$ according to $a_{bf_1} = a_{bg}\left(1 - \frac{\Delta B}{B - B0}\right)$, a_{bg} is the zero magnetic field scattering length, B_0 the Feshbach resonance magnetic field and ΔB its width.

A summary of the calculation parameters is shown at table 2.

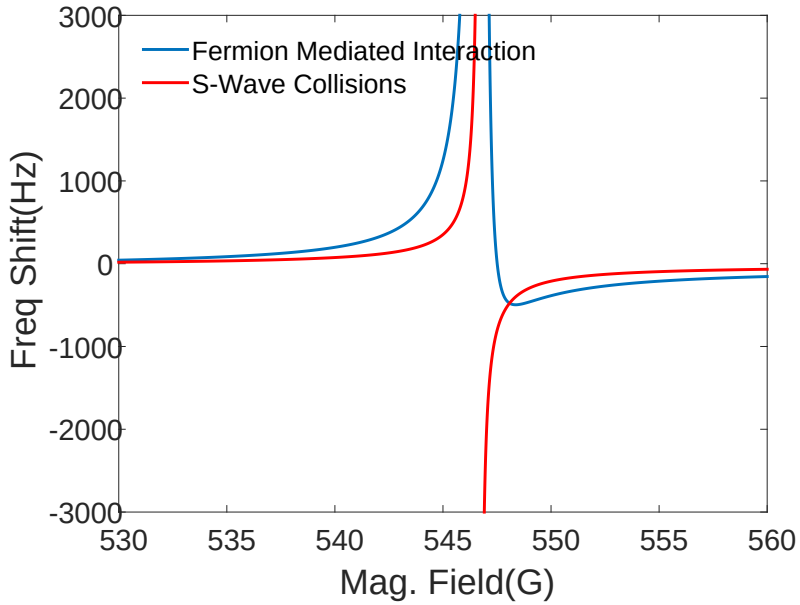

Figure 14: Mean-Field Frequency Shift Close to a Feshbach Resonance - Frequency shift for the rubidium $|1,1\rangle \rightarrow |2,2\rangle$ transition near a Feshbach resonance with fermion mediated interaction (blue) and without (red). Fermion and boson densities are constant.

Collision Rate

Atoms in a 3D harmonic trap collide at a rate $\Gamma_{col} = n\sigma \cdot \sqrt{2}v_{rms}$, n is the atoms density, σ is the collision cross section and $\sqrt{2}v_{rms}$ is the relative velocity between atoms in a trap. The cross section at low collision energies is $\sigma = 4\pi a^2$, a is the s-wave scattering length. The RMS velocity is $v_{rms} = \sqrt{\frac{8k_BT}{\mu}}$, T is the temperature, k_B- Boltzmann constant, μ - reduced mass of the colliding atoms.

In a boson-fermion mixture there are several types of collisions, we intend to measure the effect of the mediated boson-boson collisions on the collision rate of the bosons. The mediated RKKY potential is added to the normal Van der Waals interaction between the bosons. The scattering length is the low temperature limit of that potnetial so the scattering lengths are summed and the cross section is $\sigma_{bb} = 4\pi\left(a_{bb} + a_{eff}\right)^2$. A rubidium atom can undergo three types of collisions: colliding directly with other rubidium atoms, colliding with potassium atoms and mediated collisions with other rubidium atoms. A potassium atom can only collide with rubidium atoms due to Pauli exclusion principle. Thus, the collision rates for rubidium and potassium are:

$$\Gamma_{Rb} = 4\pi a_{bf}^2 v_{bf} n_f \cdot f_d + 4\pi v_b n_b \left(a_{bb} + a_{eff}\right)^2 \tag{16}$$

$$\Gamma_K = 4\pi a_{bf}^2 v_{bf} n_b \tag{17}$$

where f_d is a numerical factor that takes into account the suppression of collisions due to Pauli exclusion principle which can be approximated by $0.3 + \frac{T}{T_f}$ to first order [30]. A standard technique to measure collision rate [31] is to heat the cloud in one direction of the harmonic trap, driving it out of equilibrium, and measure the cross-dimensional thermalization rate. Heating the cloud is done by modulating the power of one of the trap beams, this gives energy to the atoms in that direction. Collisions will distribute the energy to all states and bring the cloud back to equilibrium. Out of equilibrium the momentum distribution is not an isotropic Gaussian, therefore, by looking at the aspect ratio of the cloud after a long time of flight we can measure the time it takes to get back to equilibrium. The thermalization rate is: $\tau = \frac{\Gamma_{col}}{\alpha}$ where α is the number of collisions it takes to thermalize (collisional softness) $\alpha = 2.7$ [31].

In figure 15 a calculation of the collision rate is presented, with and without the mediated interaction at zero magnetic field for different fermion densities.

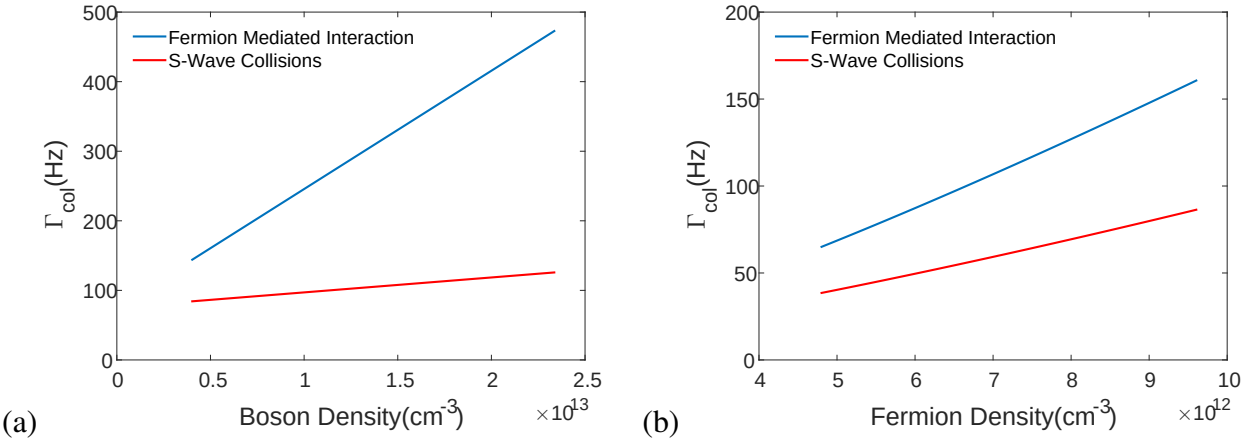

Figure 15: Collision Rate at Zero magnetic field - (a) Rubidium collision rate at zero magnetic field for different boson densities, fermion density is set at $9.6 \times 10^{12} cm^{-3}$. (b) Rubidium collision rate at zero magnetic field for different fermion densities, boson density is set at $5 \times 10^{12} cm^{-3}$. Both graphs show calculations with fermion mediated interaction (blue) and without (red).

The effect is increased close to the boson-fermion Feshbach resonance (figure 16) where the boson fermion scattering length diverges. A summary of the calculation parameters is shown at table 2.

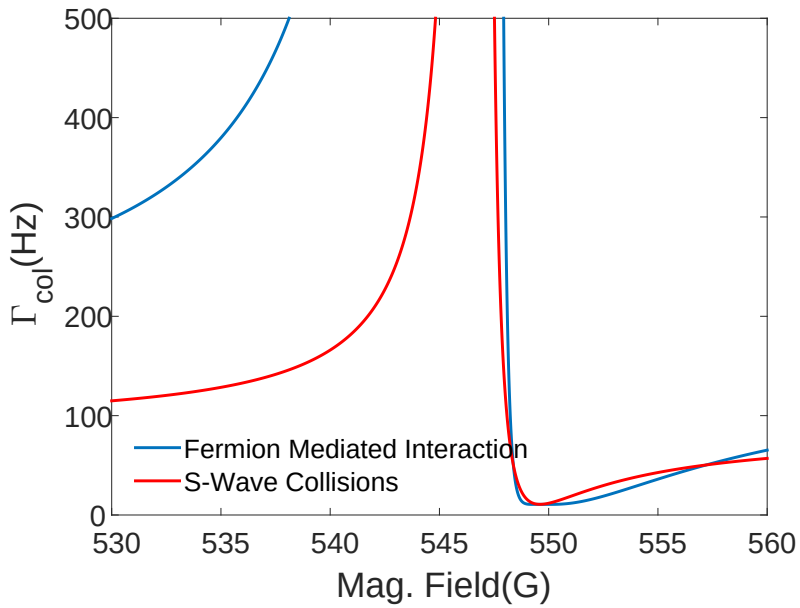

Figure 16: Collision Rate - Rubidium collision rate at zero magnetic field (left) and near a Feshbach resonance (right), with fermion mediated interaction (blue) and without (red).

Method	change n_f	change n_b	Feshbach Resonance
B	0	0	$535-555\,G$
n_f	$(5-10)\times 10^{12}cm^{-3}$	$9.6\times 10^{12}cm^{-3}$	2×10^5
n_b	$5\times 10^{12}cm^{-3}$	$(4-20)\times 10^{12}cm^{-3}$	$5\times 10^{12}cm^{-3}$
T/T_F	0.3	0.3	0.3
$\bar{\omega}$	$2\pi\times 100\,Hz$	$2\pi\times 100\,Hz$	$2\pi\times 100\,Hz$
E_F	$(0.3-0.5)\,\mu k_B$	$0.5\mu k_B$	$0.5\mu k_B$

Table 2: Calculation parameters when changing boson\fermion densities and the magnetic field close to the $^{87}Rb-^{40}K$ Feshbach resonance.

2.2 Zero Sound

Fermi liquid theory is a model of interacting fermions at low temperatures, first introduced by Lev Landau in 1956 [2]. Landau suggested taking a gas of N non-interacting fermions and turning on the interactions infinitely slowly ("adiabatically"). Under this condition, the eigenstates of the ideal gas will transform progressively into a different eigenstate of the interacting system. Each particle is now dressed by the interactions with all other particles and the low energy excitations of this new complex system is a quasiparticle with a finite lifetime. The excitations of the interacting system are defined as the deviation from the ideal momentum distribution $\delta n_{p,\sigma}=n_{p,\sigma}-n^o_{p,\sigma}$, $n^o_{p,\sigma}$ - is the non-interacting ground state momentum distribution and $n_{p,\sigma}$ is the momentum distribution of the interacting system. The theory is constructed for small deviations from the ground state ($\sum_{p,\sigma}\delta n_{p,\sigma}\ll N$) where the energy of the system can be approximated :

$$E\left[n_{p,\sigma}\right]=E_0+\sum_{p,\sigma}\varepsilon^0_{p,\sigma}\delta n_{p,\sigma}+\frac{1}{2}\sum_{p,p'\sigma,\sigma}f\left(p,\sigma;p',\sigma'\right)\delta n_{p,\sigma}\delta n_{p',\sigma'}+O\left(\delta n^3_{p,\sigma}\right) \tag{18}$$

E_0- ground state energy of the ideal gas, $\varepsilon^o_{p,\sigma}$ is the non interacting particles energy and $f\left(p,\sigma;p',\sigma'\right)=\frac{\delta^2 E}{\delta n_{p,\sigma}\delta n_{p',\sigma'}}$ measures the quasiparticle interactions. It can be related to macroscopic properties such as sound velocities or quasiparticle mass and also be related to microscopic quantities as scattering length. In the absence of magnetic fields the system is isotropic and $f\left(p,\sigma;p',\sigma'\right)$ depends only on $\sigma\cdot\sigma'$, so we can divide it to a symmetric and an antisymmetric part:

$$f\left(p,\sigma;p',\sigma'\right)=f_s\left(p,p'\right)+\left(4\sigma\cdot\sigma'\right)f_a\left(p,p'\right)\ . \tag{19}$$

Close to the Fermi surface the parameters are functions of the angle $\zeta=\cos^{-1}\left(\frac{p\cdot p'}{p_f^2}\right)$ alone and therefore may be expanded in a series of Legendre polynomials:

$$f_s\left(p,p'\right)=\sum_l f_{sl}P_l\left(\cos\zeta\right),\ f_a\left(p,p'\right)=\sum_l f_{al}P_l\left(\cos\zeta\right)\ , \tag{20}$$

f_{al}, f_{sl} are Landau parameters and are sometimes written as $F_{sl} = f_{sl} N_F$, N_F is the density of states at the Fermi energy.

One prediction of this theory is the existence of a collective mode in the collision-less regime $\omega \gg \Gamma_{col}$, ω- the frequency of the collective mode, Γ_{col} - the average collision rate. This collective mode propagates by deformation of the Fermi surface with a propagation velocity c_0 that is larger than the Fermi velocity v_f. The exact solution is defined by solving the implicit equation:

$$\frac{\lambda}{2} \log\left(\frac{\lambda+1}{\lambda-1}\right) - 1 = \frac{1}{F_{s0}} , \tag{21}$$

$\lambda = \frac{\omega}{q v_f}$ is a dimensionless parameter that sets the dispersion relation, ω is the mode frequency, q is its momentum. For $F_0 > 0$ (repulsive quasiparticle interactions) there is only one real solution with $\lambda > 1$, the zero sound wave travels faster than the Fermi velocity and is undamped. For $-1 < F_0 < 0$ (weak attractions) the solution is complex and the zero sound is damped, and for $F_0 < -1$ (strong attractions) the zero sound mode is unstable.

In [3] they show that a zero sound collective mode exists in a two component degenerate Fermi gas in an elongated harmonic trap at $T = 0$. The velocity of the zero sound mode is calculated to be:

$$c_0 = v_f^0 \left(1 + \frac{2\hbar a}{\pi r_c^2 m v_f^0}\right)^{1/2} , \tag{22}$$

a is the s-wave scattering length between the two components, v_f^0 is the Fermi velocity at the center of the trap, r_c is the size of the cloud in the tightly confined direction. We intend to excite the zero sound mode in a cloud of ^{40}K in an equal mixture of the states $\left|F = \frac{9}{2}, m_f = -\frac{9}{2}\right\rangle$, $\left|F = \frac{9}{2}, m_f = -\frac{7}{2}\right\rangle$ trapped in a 3D harmonic dipole trap. The interactions in the gas can be tuned close to a Feshbach resonance to get a small and positive scattering length, as suggested in [3]. To excite the zero sound mode a blue detuned repulsive laser beam will be turned on in the center of the trap, creating a potential barrier. We want to excite the zero sound mode without exciting the first sound mode, for this we intend to modulate the repulsive potential with a frequency $\omega \gg \Gamma_{col}$ and keep the average repulsive potential constant, similar to what was done in [32]. This should allow only the zero sound mode to propagate in the cloud. By imaging the cloud at different times we can detect the density peak moving in the cloud and measure its velocity. By comparing its velocity with the Fermi velocity and the first sound velocity $c_1 < v_f$ ($c_1 = \frac{1}{\sqrt{3}} v_f$ [33] for a free gas, $c_1 = \frac{1}{\sqrt{5}} v_f$ in the elongated trap [3]) we can recognize the zero sound mode. Another property that might be measured is the Fermi surface at the region of the excitation in the cloud. By probing only these atoms (e.g. by transferring them to a different state) we should be able to see the oscillations of the Fermi surface. To image the Fermi surface the atoms must be released for a long time of flight such that their image represents the momentum distribution.

References

[1] S De and IB Spielman. Fermion-mediated long-range interactions between bosons stored in an optical lattice. *Applied Physics B*, 114(4):527–536, 2014.

[2] LD Landau. The theory of a fermi liquid. *Soviet Physics Jetp-Ussr*, 3(6):920–925, 1957.

[3] P Capuzzi, P Vignolo, F Federici, and M P Tosi. Sound wave propagation in strongly elongated fermion clouds at finite collisionality. *Journal of Physics B: Atomic, Molecular and Optical Physics*, 39(10):S25, 2006.

[4] Jean Dalibard and Claude Cohen-Tannoudji. Laser cooling below the doppler limit by polarization gradients: simple theoretical models. *JOSA B*, 6(11):2023–2045, 1989.

[5] Markus Greiner, Immanuel Bloch, Theodor W Hänsch, and Tilman Esslinger. Magnetic transport of trapped cold atoms over a large distance. *Physical Review A*, 63(3):031401, 2001.

[6] Ettore Majorana. Atomi orientati in campo magnetico variabile. *Il Nuovo Cimento (1924-1942)*, 9(2):43–50, 1932.

[7] Heather J Lewandowski, DM Harber, Dwight L Whitaker, and EA Cornell. Simplified system for creating a bose–einstein condensate. *Journal of low temperature physics*, 132(5-6):309–367, 2003.

[8] Rudolf Grimm, Matthias Weidemüller, and Yurii B Ovchinnikov. Optical dipole traps for neutral atoms. *Advances in atomic, molecular, and optical physics*, 42:95–170, 2000.

[9] W Ketterle, DS Durfee, and DM Stamper-Kurn. Making, probing and understanding bose-einstein condensates. *arXiv preprint cond-mat/9904034*, 5, 1999.

[10] Lev P Pitaevskii and Sandro Stringari. *Bose-einstein condensation*. Number 116. Oxford University Press, 2003.

[11] M Naraschewski and DM Stamper-Kurn. Analytical description of a trapped semi-ideal bose gas at finite temperature. *Physical Review A*, 58(3):2423, 1998.

[12] Wolfgang Ketterle and NJ Van Druten. Evaporative cooling of trapped atoms. *Advances in atomic, molecular, and optical physics*, 37:181–236, 1996.

[13] Christian Ospelkaus. *Fermi-Bose mixtures : From mean-field interactions to ultracold chemistry*. PhD thesis, Universitat Hamburg, Von-Melle-Park 3, 20146 Hamburg, 2006.

[14] Michele Lynn Olsen. *Experiments with Feshbach molecules in a Bose-Fermi mixture*. PhD thesis, University of Colorado, 2008.

[15] Thorsten Best. *Interacting Bose-Fermi mixtures in optical lattices*. PhD thesis, Ph. D. Thesis, Universität Mainz, 2011.

[16] S Aubin, S Myrskog, MHT Extavour, LJ LeBlanc, D McKay, A Stummer, and JH Thywissen. Rapid sympathetic cooling to fermi degeneracy on a chip. *Nature Physics*, 2(6):384–387, 2006.

[17] Cheng-Hsun Wu et al. *Strongly interacting quantum mixtures of ultracold atoms*. PhD thesis, Massachusetts Institute of Technology, 2013.

[18] Walther Gerlach and Otto Stern. Der experimentelle nachweis der richtungsquantelung im magnetfeld. *Zeitschrift für Physik A Hadrons and Nuclei*, 9(1):349–352, 1922.

[19] M. H. Anderson, J. R. Ensher, M. R. Matthews, C. E. Wieman, and E. A. Cornell. Observation of bose-einstein condensation in a dilute atomic vapor. *Science*, 269(5221):198–201, 1995.

[20] Melvin A Ruderman and Charles Kittel. Indirect exchange coupling of nuclear magnetic moments by conduction electrons. *Physical Review*, 96(1):99, 1954.

[21] Tadao Kasuya. A theory of metallic ferro-and antiferromagnetism on zener's model. *Progress of theoretical physics*, 16(1):45–57, 1956.

[22] Kei Yosida. Magnetic properties of cu-mn alloys. *Physical Review*, 106(5):893, 1957.

[23] Francesca Ferlaino, Chiara DErrico, Giacomo Roati, Matteo Zaccanti, Massimo Inguscio, Giovanni Modugno, and Andrea Simoni. Feshbach spectroscopy of a k- rb atomic mixture. *Physical Review A*, 73(4):040702, 2006.

[24] Kurt Gibble and Steven Chu. Laser-cooled cs frequency standard and a measurement of the frequency shift due to ultracold collisions. *Physical review letters*, 70(12):1771, 1993.

[25] DM Harber, HJ Lewandowski, JM McGuirk, and EA Cornell. Effect of cold collisions on spin coherence and resonance shifts in a magnetically trapped ultracold gas. *Physical Review A*, 66(5):053616, 2002.

[26] Christopher J Foot. *Atomic physics*. Oxford University Press, 2004.

[27] Daniel A Steck. Rubidium 87 d line data, 2001.

[28] Yvan Sortais, Sebastien Bize, Michel Abgrall, Shougang Zhang, Christophe Nicolas, Cipriana Mandache, Pierre Lemonde, Pagani Laurent, Giorgio Santarelli, Noël Dimarcq, et al. Cold atom clocks. *Physica Scripta*, 2001(T95):50, 2001.

[29] M Egorov, B Opanchuk, P Drummond, BV Hall, P Hannaford, and AI Sidorov. Measurement of s-wave scattering lengths in a two-component bose-einstein condensate. *Physical Review A*, 87(5):053614, 2013.

[30] B DeMarco, SB Papp, and DS Jin. Pauli blocking of collisions in a quantum degenerate atomic fermi gas. *Physical Review Letters*, 86(24):5409, 2001.

[31] CR Monroe, Eric A Cornell, CA Sackett, CJ Myatt, and CE Wieman. Measurement of cs-cs elastic scattering at t= 30 μk. *Physical review letters*, 70(4):414, 1993.

[32] Leonid A Sidorenkov, Meng Khoon Tey, Rudolf Grimm, Yan-Hua Hou, Lev Pitaevskii, and Sandro Stringari. Second sound and the superfluid fraction in a fermi gas with resonant interactions. *Nature*, 498(7452):78–81, 2013.

[33] Philippe Nozières and David Pines. *Theory of quantum liquids*. Westview Press, 1999.